Glacier loss and vegetation expansion alter organic and inorganic carbon dynamics in high-mountain streams

Andrew L. Robison[1], Nicola Deluigi[1], Camille Rolland[1], Nicola Manetti[1], and Tom Battin[1]

[1]River Ecosystems Laboratory, Center for Alpine and Polar Environmental Research (ALPOLE), Ecole Polytechnique Fédérale de Lausanne (EPFL), Lausanne, Switzerland.

Corresponding author: Andrew L. Robison, andrew.robison@epfl.ch

Abstract

High-mountain ecosystems are experiencing acute effects of climate change, most visibly through glacier recession and the greening of the terrestrial environment. The streams draining these landscapes are affected by these shifts, integrating hydrologic, geologic, and biological signals across the catchment. We examined the organic and inorganic carbon dynamics of streams in four Alpine catchments in Switzerland to assess how glacier loss and vegetation expansion are affecting the carbon cycle of these high-mountain ecosystems. We find that organic carbon concentration and fluorescence properties associated with humic-like compounds increase with vegetation cover within a catchment, demonstrating the increasing importance of allochthonous dissolved organic carbon sources following glacier retreat. Meanwhile, streams transitioned from carbon dioxide sinks to sources with decreasing glacier coverage and increased vegetation coverage, with chemical weathering and soil respiration likely determining the balance. Periods of sink behavior were also observed in non-glaciated streams, possibly indicating chemical consumption of carbon dioxide could be more common in high-mountain, minimally vegetated catchments than previously known. Together, these results demonstrate the dramatic shifts in carbon dynamics of high-mountain streams following glacier recession, with significant changes to both the organic and inorganic carbon cycles. The clear link between the terrestrial and aquatic zones further emphasizes the coupled dynamics with which all hydrologic and biogeochemical changes in these ecosystems should be considered, including the carbon sink or source potential of montane ecosystems.

Short summary

Climate change is affecting mountain ecosystems intensely, including the loss of glaciers and the uphill migration of plants. How these changes will affect the streams draining these landscapes is not well known. We sampled streams across a gradient of glacier and vegetation over in Switzerland and found glacier loss reduced the carbon dioxide sink from weathering, while vegetation cover increased organic

Keywords

Streams, climate change, glaciers, carbon dioxide, organic carbon

1. Introduction

The effects of climate change on high-mountain areas are dramatic, with temperatures increasing approximately twice as quickly as in lower elevation areas (IPCC, 2021). With glacial retreat, the streams draining these landscapes are experiencing significant change in the timing, magnitude, and source of flows (Kneib et al., 2020; Mackay et al., 2019). The terrestrial environment is also shifting with the expansion of vegetation spatially (i.e., to higher elevations) and temporally (i.e., longer growing season), which thereby impact the hydrology, biogeochemistry, and ecology of catchment streams (Knight and Harrison, 2014; Brighenti et al., 2019). In the Swiss Alps, recent work has highlighted the rapid "greening" of high-mountain areas and decreasing snow and ice cover (Rumpf et al., 2022). While the implications of climate change for terrestrial ecosystems have been examined broadly (Finstad et al., 2016), the impact these changes will exert on the streams draining these landscapes is much less explored (Beniston et al., 2018). Given the global extent and integral role of streams in connecting high-mountain areas with downstream ecosystems (Milner et al., 2017), exploring how these landscape alterations will affect the carbon dynamics of streams is critical to contextualize their role in the global cycle (Horgby et al., 2019c).

High-mountain streams are tightly linked to the catchment they drain (Milner et al., 2009; Brighenti et al., 2019). In particular, the presence of glaciers dominates stream hydrology (Kneib et al., 2020), with significant biogeochemical and ecological implications. For example, as glaciers generally provide the majority of water to their proglacial streams, solute concentration and flux are frequently controlled by the contents and magnitude of glacier melt water (Bergstrom et al., 2021). For example, dissolved organic carbon (DOC) ice-locked within glaciers can be the dominant source of DOC to the proglacial stream upon melting (Colombo et al., 2019). The lability of this glacier-derived DOC is often high, serving as a major source of carbon fueling downstream metabolism (Hood et al., 2009). Glaciers are also associated with high rates of geochemical weathering, both underneath the glacier (Anderson et al., 1997) and in the proglacial stream (St. Pierre et al., 2019). The weathering of both carbonate and silicate minerals can consume atmospheric carbon dioxide (CO_2), whereby CO_2 dissolved in water is converted to bicarbonate through these reactions (Donnini et al., 2016). These reactions involve significant transformations of dissolved inorganic carbon (DIC) and potentially consume large amounts of CO_2 in the process (Hodson et al., 2000).

As glaciers shrink, there is generally a concomitant increase in soil development and vegetation cover within catchments (Guelland et al., 2013). Higher vegetation cover and soil development provides a pool of organic carbon for export to the streams (Garcia et al., 2015). From this change, increases in stream DOC concentration are likely. Indeed, increased DOC in aquatic ecosystems globally has been directly linked to the greening of the terrestrial landscape (Finstad et al., 2016). Elevated aquatic DOC has implications for ecosystem respiration, productivity, and water quality (Roulet and Moore, 2006; Hongve et al., 2004). This change in DOC source also implies changes to the quality of stream organic matter (Zhou et al., 2019), which could further alter stream metabolic regimes by promoting heterotrophy (Bernhardt et al., 2017; Duarte and Prairie, 2005; Boix Canadell et al., 2020). In terms of inorganic carbon, soils frequently represent the dominant source of CO_2 to streams, as the products of soil respiration are transported to the stream via groundwater (Hotchkiss et al., 2015). Thus, as soils develop and allow for the expansion of vegetation in mountain catchments, emissions of CO_2 from the aquatic system may be promoted as the products of soil respiration are transported to the stream and emitted.

Given these complex relationships, consideration of both glacial influence and the terrestrial environment at-large is key to fully contextualize how climate change may alter carbon flows to and from mountain streams. Moreover, both the organic and inorganic carbon components must be evaluated to complete this cycle, providing perspective on the relative

influence of different catchment properties. In this study, we aim to evaluate landscape effects on dissolved organic and inorganic carbon dynamics in high-mountain streams across a glacial, vegetation, and elevation gradient. By comparing dissolved carbon concentration and fluxes across these gradients, we can directly assess the relative impact of glacial retreat and catchment greening. We hypothesized the presence of glaciers would drive CO_2 consumption (St. Pierre et al., 2019), and the loss of glacier influence would elevate the role of catchment soils as a source of CO_2 (Crawford et al., 2015). We also expected these landscape transformations would increase the role of allochthonous organic to the stream (Fasching et al., 2016), with consequential changes to the quality of organic matter.

2. Methods

Samples of DOC and DIC were collected, as well as *in situ* sensor measurements of dissolved carbon dioxide (pCO_2) in 12 streams in the high-mountain area of the western Swiss Alps over five years, from 2016 to2020. The sampling locations covered a broad range of catchment glacier coverage, vegetation coverage, and elevation, providing for a space-for-time substitution approach in which streams draining lower elevation, lower glacier cover, and higher vegetation cover catchments represent potential future conditions of higher elevation, higher glacier cover, and lower vegetation cover catchments. With this spatial design, we can to evaluate how these carbon constituents may evolve with ecosystem processes following anthropogenic climate change. Consideration of various other water quality and catchment properties (e.g., dissolved oxygen, inorganic carbon isotopes, dissolved organic matter fluorescence) provides further insight on changes in the relative contribution of geochemical weathering, in-stream processes, and terrestrial inputs within these streams.

2.1 Site description

Our 12 stream sampling locations were equally distributed within Vallon de Nant, Champéry, Valsorey and Val Ferret, four catchments in the western Swiss Alps (Figure 1). These sites are part of the METALP project (https://metalp.epfl.ch), which has been described extensively in previous studies (Ulseth et al., 2019; Boix Canadell et al., 2019; Horgby et al., 2019c) and where numerous hydrological and biogeochemical parameters have been monitored since 2016. The drainage areas vary from 0.31 km^2 to 23.2 km^2, and mean catchment elevation from 1778 m to 2892 m (Table 1). Vegetation cover is highest at lower elevations, and ranged from approximately 94% to 21% coverage of the catchment.

Figure 1: Map of the 12 study sites within four catchments of the Alps in southwestern Switzerland (glacial cover and stream network from swissTLM3D; swisstopo).

The geology of the Champéry and Vallon de Nant catchments is dominated by the presence of limestones, calcareous shales, and flysch (Burri et al., 1999). Val Ferret is characterized by limestones and sandstones showing pronounced schistosity, while Valsorey is underlain primarily by a metamorphic lithology that distinguishes with gneisses, crystalline shales, and blue-grey schists. Additionally, in Valsorey, glacial cover accounts for about one third of the total surface, with the blue-grey schists most prominent at high elevations beneath and near the glaciers. Soils in this region are generally young, poorly developed leptosols and fluvisols (Egli et al., 2010), with organic content that increases at lower elevations (Hoffmann et al., 2014). While soil organic content has not been measured in these catchments, measurements in nearby areas of the Swiss Alps have observed soil organic content ranging from < 0.1 kg C m^{-2} in soils around 2150 m elevation to around 2.0 kg C m^{-2} at 1000 m elevation (Hoffmann et al., 2014; Egli et al., 2010).

Table 1: Catchment characteristics.

2.2 Grab sampling and sensor measurements

Grab sampling of various physical and chemical parameters were made at all sampling sites at approximately monthly intervals during the snow-free season. These parameters include DOC, dissolved organic matter (DOM) fluorescence, major ions, pCO_2, DIC, and alkalinity. The analysis of these analytes has been described previously (Horgby et al., 2019b; Boix Canadell et al., 2019). Concentrations of major anions (Ca^{2+}, Mg^{2+}, K^+, and Na^+) and cations (SO_4^{2-}, NO_3^-, and Cl^-) were measured on streamwater filtered through 0.22-µm filters (Mixed Cellulose Ester) using ion chromatography (Metrohm 930 Compact IC Flex; Aargau, Switzerland).

Samples for the quantification of DOC and DOM fluorescence are filtered through pre-combusted 0.45 µm GF/F filters (Whatman) into acid-washed and pre-combusted 40 mL amber glass vials. Samples are kept refrigerated and analyzed for concentration within 24 h from collection. DOC concentration was measured using a Sievers M5310C TOC Analyzer (GE Analytical Instruments, New York, USA) with an accuracy of ±2% µg C L^{-1}, a precision of <1% relative standard deviation, and a detection limit of 22 µg C L^{-1}). Samples were taken in triplicates and the mean concentration was used, with outliers removed if the concentration exceeds three standard deviations from the mean. Calibration standards ranged from 0.05 to 1 mg C L^{-1}. DOM fluorescence excitation-emission matrices (EEMs) were created by measuring fluorescence intensity of samples within a 1 cm cuvette across a range of excitation (240–450 nm, 2 nm increment) and emission (211.19–620.23 nm, 2 nm increments) wavelengths using an Aqualog® optical spectrometer (Horiba, Kyoto, Japan). Validation scans are performed prior to sample analysis to validate instrument performance, such as measuring the water Raman signal-to-noise ratio and emission calibration using a sealed, standard cuvette of Milli-Q water (Type 1 LRW) to ensure the Raman peak position is at 297 nm ± 1 nm. Milli-Q water was used as a blank, which was used to remove background fluorescence from the spectra. Absorbance was also measured within a 10 cm cuvette with a Perkin Elmer Lamba 850 spectrophotometer (Massachusetts, USA).

Duplicate samples for dissolved inorganic carbon (DIC) concentration and the relative stable carbon isotopic composition (δ^{13}C-DIC) were filtered through 0.2 µm membrane filters into acid-washed 12 mL glass exetainer vials and stored refrigerated until analysis. Two mL of sample were injected into synthetic air-filled, septum capped~~,~~ 12 mL exetainer vials containing 200 µL 85% phosphoric acid to convert all DIC to gaseous CO_2. The resulting gas phase was then analyzed on the CRDS-SSIM2 equipped with a Small Sample Isotope Module 2 (CRDS-SSIM2, Picarro Inc., California, USA) and converted into DIC concentration.

Additionally, each monitoring station was instrumented with sensors measuring physical and chemical parameters of the water or air at a 10 min frequency, including water temperature, dissolved oxygen, carbon dioxide (pCO_2), and depth. Specifications, calibration and maintenance procedures of these sensors have been described previously (Horgby et al., 2019c; Boix Canadell et al., 2020). Stream pCO_2 was measured using a CARBOCAP® GMP252 probe (Vaisala, Vantaa, Finland) within a porous polytetrafluoroethylene (ePDFE) semi-permeable membrane. The probes were then protected with a fine-grained mesh, and a metal casing. Raw data were adjusted according to the manufacturer's recommendations for barometric pressure and water temperature. All pCO_2 sensors were tested in the laboratory using certified gas mixtures of CO_2 diluted in synthetic air to final concentrations of 0, 400 and 2000 ppmv prior to deployment.

Discharge was calculated using rating curves relating water depth to discharge (Boix Canadell et al., 2021), where direct measurements of discharge were made using slug injections of sodium chloride (NaCl) as a conservative tracer (Gordon et al., 2004).

Additionally, when stream conditions allowed, 10 random measurements of stream depth were collected to provide a measure of average stream morphology to compare with measurements recorded by the sensor installed on the streamside.

2.3 CO_2 saturation and efflux

From the 10-minute sensor data, the daily median concentration of CO_2 was found for all sample locations during the monitoring period (Horgby et al., 2019c). The saturation and efflux for these values were then estimated using measurements of stream water temperature, and estimates of barometric pressure, atmospheric concentration of CO_2, and gas exchange velocity. Barometric pressure was obtained from the MeteoSwiss weather station network (Swiss Federal Office and Meteorology and Climatology). The Col du Grand St Bernard station (elevation 2473 m a.s.l.) was used for the Valsorey and Ferret catchments, while the Evionnaz station (482 m a.s.l.) and Les Diablerets (2964 m a.s.l.) stations were used for Champéry and Vallon de Nant stations. Barometric pressure at each monitoring stations (P_{site}, mbar) was adjusted for site-specific elevation and temperature following:

$$P_{site} = P_0 \exp\left(\frac{-gM(h-h_0)}{RT}\right), \quad (1)$$

where P_0 (mbar) is the barometric pressure measured at the MeteoSwiss station, h_0 and h (m) are the altitude of the meteorological and at the monitoring stations, respectively, g is the gravity acceleration (9.81 m s^{-2}), M the molar mass of air (0.0289644 kg mol^{-L}) and R the universal gas constant (8.31432 J mol^{-1} K^{-1}). The temperature of air T_{air} (°C) at the METALP stations is estimated through the temperature T_0 (°C) measured at the MeteoSwiss station, where the regional temperature gradient $\Delta T/\Delta h$ is set to -0.54 °C/100 m, obtained from air temperature data collected during the period 1990-2020 by the Evolène-Villa (1427 m a.s.l.) and the Montana (1825 m a.s.l.) weather stations (MeteoSwiss; Deluigi et al., 2017),

$$T_{air} = T_0 - \left((h - h_0) \cdot \frac{\Delta T}{\Delta h}\right). \quad (2)$$

Sensor measurements of $pCO_{2,raw}$ (ppm) were then adjusted to site-specific temperature and barometric pressure following the ideal gas law:

$$pCO_{2,corr} = pCO_{2,raw} \cdot \frac{P_{site}}{1013} \cdot \frac{298}{T_{water}}, \quad (3)$$

where P_{site} (mbar) is the barometric pressure at each location and T_{water} (K) is the measured water temperature. Dissolved CO_2 concentration ($CO_{2,water}$, µmol L^{-1}) was then derived by multiplying the corrected $pCO_{2,corr}$ with Henry's constant K_H (mol L^{-1} atm^{-1}) at each site,

$$CO_{2,water} = pCO_{2,corr} \cdot K_H. \quad (4)$$

K_H is a function of the water temperature in Kelvins (T_{water}) with A is 108.3865, B is 0.01985076, C is -6919.53, D is -40.4515, E is 669365 according to Plummer and Busenberg (1982),

$$K_H = 10^{A+B\cdot T_{water}+\frac{C}{T_{water}}+D\cdot\log_{10}(T_{water})+\frac{E}{T_{water}^2}}. \quad (5)$$

A corresponding dissolved equilibrium concentration of CO_2 ($CO_{2,sat}$, μmol L^{-1}) was calculated for each sensor measurements at each site using an estimate of daily mean atmospheric CO_2 ($CO_{2,air}$),

$$CO_{2,sat} = CO_{2,air} \cdot K_H, \quad (6)$$

by adjusting measurements of CO_2 concentration at Jungfraujoch (freely available at http://www.climate.unibe.ch) for differences in barometric pressure and temperature,

$$CO_{2,air} = CO_{2,Jungfrau} \cdot \frac{P_{site}}{P_{Jungfraujoch}} \cdot \frac{T_{Jungfraujoch}}{T_{Site}}. \quad (7)$$

The standard gas transfer velocity (k_{600}, m d^{-1}) was calculated using the relationships developed by Ulseth et al. (2019) and extrapolated from the same 12 streams in this study:

$$\ln(k_{600}) \text{ for } eD > 0.02 = 1.18 \cdot \ln(eD) + 6.63 \quad (8)$$
$$\ln(k_{600}) \text{ for } eD < 0.02 = 0.35 \cdot \ln(eD) + 3.10 \quad (9)$$

where eD is the stream energy dissipation rate (m^2 s^{-3}), which is obtained by multiplying the gravity acceleration (9.81 m s^{-2}) with slope (S, unitless) and stream flow velocity (V, m s^{-1}),

$$eD = g \cdot S \cdot V \quad (10)$$

Velocity was calculated according to the hydraulic geometry scaling proposed by (Horgby et al., 2019c) for these streams,

$$V = 0.668 \cdot Q^{0.365}, \quad (11)$$

where Q is discharge (m^3 s^{-1}). To convert k_{600} to k_{CO2} (Eq. 11) we used the temperature dependent Schmidt scaling according to (Wanninkhof, 2014),

$$Sc_{CO_2} = 1923.6 - 125.06 \cdot T_W + 4.3773 \cdot T_W^2 - 0.85681 \cdot T_W^3 + 0.00070284 \cdot T_W^4 \quad (12)$$

$$k_{CO_2} = \frac{k_{600}}{\left(\frac{600}{Sc_{CO_2}}\right)^{-0.5}} \quad (13)$$

The CO_2 efflux (F_{CO2}, g CO_2-C m^{-2} d^{-1}) was then calculated as,

$$F_{CO_2} = k_{CO_2} \times \left(CO_{2,water} - CO_{2,sat}\right). \quad (14)$$

2.4 PARAFAC modelling

Parallel factor analysis (PARAFAC) modelling of fluorescence excitation-emission matrices (EEMs) was used to identify and determine the main fluorescence components of DOM present across collected water samples and was conducted using the R packages *staRdom* (Pucher et al., 2019) and eemR (Massicotte, 2019). Pre-processing of EEMs was necessary prior to PARAFAC development (Murphy et al., 2013; Stedmon & Bro, 2008). Briefly, spectra were corrected for instrument-specific effects, blank subtraction, inner-filter effects. First- and second-order Rayleigh scattering was removed and corrected EEMs

normalized to Raman units (Murphy et al., 2010). A total of 220 samples were included for model development. The final PARAFAC model was validated using split-half analysis. The resulting components were compared to previously published fluorescence components from aquatic ecosystems in the OpenFluor database (Murphy et al., 2014).

2.5 Statistical analyses

All statistical analyses were performed in MATLAB and Statistics Toolbox Release 2021a (MathWorks, Massachusetts, USA). Differences in concentration or saturation between groups of streams was investigated using Kruskal-Wallis tests. Simple linear regression was used to evaluate relationships between DOC concentration or CO_2 saturation with catchment properties and water quality parameters. The Pearson correlation coefficient (r) and coefficient of determination (r^2) were used to determine the strength of correlations, with the Pearson correlation coefficient used to show the direction of interaction.

The highly correlated nature of potential explanatory variables limited interpretability for CO_2 saturation, thus we used partial least squares (PLS) regression to identify variables important for predicting median CO_2 saturation at each site. PLS is a method which is well-designed for datasets with many collinear predictor variables and when the number of observations is small relative to the number of predictor variables (Wold et al., 1984; Carrascal et al., 2009; Nash and Chaloud, 2011). Here, our response variable is the median CO_2 saturation of each stream location, and 39 predictor variables (standardized within the PLS model) are included (Table S1).

A Monte-Carlo cross-validation method assessed the predictive ability of the resulting PLS model, where the model was fitted with a sub-sample of data. The calibration validation ratio was set to 0.8, following Onderka et al. (2012), then the resulting fitted models were tested on the validation set. This process was repeated 500 times. The mean cross-validated goodness of prediction (Q^2) was then compared to the original model fit (R^2Y). The strength of each predictor variable within the model was then analyzed using variable importance in the projection (VIP), where highly important variables had VIP > 1.0 (Eriksson et al., 2001). Additionally, moderately important ($0.8 < VIP < 1.0$) or less influential ($VIP < 0.8$) variables were identified.

Finally, catchment areal fluxes of CO_2, DIC, and DOC were calculated using catchment area and estimates of stream surface area. We focus on the snow-free period, July 1 through October 31 (Deluigi et al., 2017), to exclude snow cover as a confounding factor affecting gas exchange. Concentration and gas exchange rates are considered constant within subcatchments. An estimation of the network stream area was computed as the product of the stream length and width during this snow free period. Perennial stream length was extracted from the large-scale topographic landscape model of Switzerland (swissTLM3D) and compared to a 2m-resolution DEM stream network (swissALTI3D). Considering the complexity of the network and its remoteness, stream widths were estimated on aerial images with a 25 cm pixel resolution, with a minimum of one width measurement per stream order. An average of 187 width estimates were made per catchment. The calculation of areal flux for CO_2 is particularly uncertain as stream surface area (Paillex et al., 2020), gas exchange (Ulseth et al., 2019), and pCO_2 (Horgby et al., 2019b) are each highly dynamic in high-mountain river networks. Thus, these estimates remain approximations intended to provide perspective on the relative balance of dissolved carbon constituents in these stream networks rather than robust calculations of flux. We consider CO_2 as a vertical flux, either into or out of the stream, while DOC and DIC are downstream fluxes. The downstream DIC flux inherently includes downstream transport of CO_2.

3. Results

3.1 Dissolved carbon concentrations

The overall median concentration of DOC was 0.22 mg C L^{-1}, with site specific median concentrations ranging from 0.12 mg C L^{-1} at the upper Val Ferret site (FEU), to 0.45 mg C L^{-1} in the tributary stream at Vallon de Nant (RIC) (Figure 2a; Table 2). All measured DOC concentrations (212 samples) were below 1.00 mg C L^{-1}. From simple linear regression, median DOC concentration at a site varied most strongly with catchment vegetation cover (r = 0.76), δ^{13}C-DIC values (r = -0.75), and catchment glacier cover (r = -0.53).

Table 2: Median concentration of DOC and DIC, percent saturation of CO_2 and O_2, and isotopic composition of DIC for the 12 sites. Concentration and isotopic composition are summarized from grab samples, while CO_2 and O_2 saturation are summarized from sensor data.

Figure 2: Boxplots of a) DOC and b) DIC concentration (mg L^{-1}) from grab samples, and c) CO_2 saturation (%) derived from sensor measurements.

Concentrations of DIC were generally greater and more varied than DOC, with an overall median DIC concentration of 1.77 mg C L^{-1} across 191 samples, ranging between 0.79 and 2.65 mg C L^{-1} (Figure 2b). DIC concentration was most strongly correlated to decreasing mean catchment elevation (r = -0.67), with the three relatively high elevation Valsorey locations exhibiting significantly lower median concentrations than the other nine sites ($p < 0.01$). The median δ^{13}C-DIC value across sites was -6.14‰ (Table 2). The Champéry locations exhibited the most depleted δ^{13}C-DIC values (median = -9.28‰), which were significantly lower than the remaining nine streams ($p = 0.02$).

Across all streams, the median saturation of CO_2 was 95.1%, with the lowest median saturation of 68.1% measured at the upstream location at Valsorey (VAU) and the highest median saturation of 137% measured at the upstream location at Val Ferret (FEU; Figure 2c). All sites exhibited periods of oversaturation and undersaturation, except for VAU, where undersaturation was always observed. CO_2 saturation was significantly positively correlated with specific conductivity, alkalinity, DIC, and calcium, and negatively correlated with glacier coverage and specific UV absorbance at 254 nm ($SUVA_{254}$). However, the variance explained by any of these individual variables was low ($r^2 < 0.3$). A three-component PLS model was extracted which explained roughly 49% of the variance in median CO_2 saturation ($R^2Y = 0.49$), with moderate predictive power ($Q^2 = 0.42$). Ten variables were deemed highly influential (VIP > 1). These include catchment characteristics of mean catchment elevation, catchment area, glacier cover, and vegetation cover. Additionally, water quality parameters deemed influential were specific conductivity, sulfate and calcium concentration, total suspended solids, and discharge. Additionally, DOC was identified as a moderately influential variable.

Dissolved oxygen saturation was much less variable than CO_2 across sites, with median values between 98% and 100% and periods of over- and undersaturation for all sites (Table 2). Similarly, the interquartile range of CO_2 saturation across all sites was large, 38.1%, when compared to that of dissolved oxygen, 2.3%. The major cation across sites was Ca^{2+}, and the major anion was SO_4^{2-} (Table S2). The log ratios of Mg^{2+} and Ca^{2+} to SO_4^{2-} are similar across sites (Figure 3), clustering closest to carbonate end-members (Torres et al., 2017). Within larger catchments, only the tributary site within the Val Ferret catchment (PEU) differs significantly from the main stem stream locations.

Figure 3: Stoichiometry of dissolved ion in the twelve study streams and a data base of 95 glacier-fed streams (Torres et al., 2017). The range of each lithological end-member are

shown by the boxes. The tributary stream in the Val Ferret catchment (PEU) is shown as it is clearly distinguished from the main stream locations.

3.2 PARAFAC modelling results

PARAFAC modelling resulted in a four-component model (Figure S1). In comparing these components to the OpenFluor database, the first (C1) and second component (C2) are likely of terrestrial humic origin, while the third (C3) and fourth (C4) are proteinaceous, likely of microbial origin (Kida et al., 2019). The components resemble those reported from other freshwater and glacial environments (e.g., Spencer et al. 2014, Imbeau and Vincent 2021, Kida et al. 2021). When compared to EEM fluorophore peaks assigned by Coble et al. (1990, 1998), C1 appears to reflect the A and C peaks which are associated with humic-like compounds from biodegradation of terrestrial plant matter, while C2 contains peak M, which is linked to humic-like compounds related to primary production. Similarly, C3 appears like the T peak and C4 the B peak, both of which are suggested to be proteinaceous compounds of microbial origin. In general, the humic-associated components were found in greater intensity (median = 0.038 and 0.024 RU for C1 and C2, respectively) than the protein-associated components (median = 0.019 and 0.008 RU for C3 and C4, respectively). Both of the humic-associated components were significantly positively correlated with DOC concentration across all sites, C1 ($r = 0.86$) and C2 ($r = 0.69$) (Figure 4). The protein-associated peaks showed little correlation with DOC concentration ($r^2 \leq 0.2$).

Figure 4: Intensity of the four components within the PARAFAC model against DOC concentration from grab samples, with catchment vegetation cover shown by color. a) Component 1 and b) component 2 represent humic-like compounds while c) component 3 and d) component 4 represent proteinaceous compounds. The coefficient of determination (r^2) is shown for each linear regression.

3.3 Catchment carbon fluxes

Total areal fluxes of dissolved carbon during the snow-free period ranged from -0.027 to 0.052 g C m^{-2} catchment area d^{-1}, at the upstream Valsorey and downstream Champéry locations, respectively (Figure 5). Considering absolute fluxes, CO_2 was the largest component of the dissolved carbon flux, contributing a median of 67%. DIC contributed 29% to the total carbon flux, and DOC contributed the least (4%). Negative net fluxes of C represent occasions when the stream is estimated to be a net sink of CO_2, and this sink exceeds the downstream transport of DOC and DIC. This occurred in only a single catchment (Valsorey).

Figure 5: Estimated annual fluxes of the dissolved carbon components (CO_2, DOC, and DIC) normalized for catchment area.

4. Discussion

Comparing the dissolved carbon constituents in stream water within the space-for-time framework provided by these 12 study sites highlights how the changing nature of high-mountain catchments will have dramatic effects on the stream carbon cycle. There is a clear difference in DOC between higher and lower elevation sites, likely as allochthonous carbon becomes more important with increasing vegetation cover at lower elevation. The saturation of CO_2 appears related to these DOC inputs, not only as a potential source of carbon for in-stream respiration, but also as an indicator of an increasing importance of soil-derived CO_2 to the stream. Geochemical weathering remains a significant sink of CO_2, most strongly in

glaciated catchments. However, the relevance of geochemical weathering to the CO_2 budget is not limited to glaciated catchments, as periods of under-saturation were observed in non-glaciated streams. The dissolved carbon dynamics of montane streams are thus critically tied to the dissolved carbon dynamics of high-mountain streams.

4.1 Increasing allochthonous DOC in high-mountain streams

The observed relationships between DOC concentration and catchment vegetation cover, and even more strongly the humic-like components of the DOM pool, suggest allochthonous sources drive the increase in DOC concentration across these high-mountain streams. Higher stream DOC concentration has been attributed to greater terrestrial inputs and increasing vegetation cover (Zhou et al., 2019; Pain et al., 2020), as well as decreasing glacier influence (Fellman et al., 2010). The routing of water through catchment soils should thus play an increasingly large role in determining the timing and magnitude of allochthonous carbon export to high-mountain streams generally. For example, as the terrestrial environment becomes a more important source of DOC to streams, so too should hydrologic transport (Gómez-Gener et al., 2021). For example, in our study streams, DOC export has been shown to be strongly related to discharge patterns, with snowmelt mobilizing additional DOC compared to other seasons (Boix Canadell et al., 2019; Boyer et al., 1997). Similarly, rain events should then be related to increased humic-like DOM inputs from terrestrial sources as transport from hillslope to stream is amplified (Fasching et al., 2016). While the indication of allochthony from DOM optical properties is imperfect (Begum et al., 2023; Guillemette and del Giorgio, 2012), the complementary DOC concentration patterns with vegetation cover and elevation reinforce the interpretation of these data.

Vegetation cover, as used in this study, serves as a broad indicator of soil development within these catchments, where accumulation of soil material allows for vegetation expansion (Hagedorn et al., 2019; Henne et al., 2011). The use of vegetation cover as a proxy for soil development following deglaciation is accurate in early successional stages (Klaar et al., 2014), which is true of the catchments in this studies. The development of soil, as indicated by increasing vegetation cover, can increase the pool of organic carbon in glacier forelands (Wietrzyk-Pełka et al., 2020; Dümig et al., 2011; Egli et al., 2010), which can then be a source or organic carbon to the proglacial stream (Zah and Uehlinger, 2001). For example, in glacier fed streams in Canada, stream DOC concentration increased with catchment soil development (slope ≈ 0.2 mg C L^{-1} soil % catchment $area^{-1}$; Lafrenière and Sharp, 2004), similar to our relationship with vegetation (slope = 0.05 mg C L^{-1} vegetation % catchment $area^{-1}$). Either of these metrics, vegetation or soil, are indicative of significant catchment change with implications for terrestrial-aquatic carbon transfers.

Considering the greening of the terrestrial environment in the Alps (Rumpf et al., 2022), it follows that the streams draining these landscapes may be expected to experience an increase in DOC concentration of terrestrial origin. Our results support this hypothesis, in which stream DOC concentration and the humic-like components likely of allochthonous origin increase with catchment vegetation cover. These changes have potentially important implications for these streams as well as their downstream ecosystems, from altering metabolic regimes by promoting heterotrophy (Hall et al., 2016), limiting primary productivity (Kritzberg et al., 2019), and causing higher drinking water production costs (Hongve et al., 2004). Even while relatively low in concentration, the foundational physical, biochemical, and ecological nature of DOC within streams magnifies the impact of these changes in DOC concentration and highlight the substantial consequences of vegetation expansion following glacial retreat.

4.2 Terrestrial biogeochemical processes drive aquatic CO_2 saturation patterns

With regards to CO_2, extensive periods of undersaturation are relatively rare in riverine systems, but are likely explained by geochemical weathering (St. Pierre et al., 2019). In our study, the isotopic signature of DIC provides the primary evidence of geochemical weathering, where depleted δ^{13}C-DIC values (approximately -9 to -3‰) relative to atmospheric equilibrium are indicative of weathering (Skidmore et al., 2004). This agrees well with glacier-fed streams in Alaska (-7 to 0‰; St. Pierre et al. 2019), and mineral sources of DIC have been highlighted in Swiss high-mountain streams previously (Horgby et al., 2019c). Furthermore, the PLS model results also distinguish influential factors related to the products of weathering (i.e., specific conductivity, sulfate and calcium concentration) or which affect the rate of weathering (i.e., glacier cover, runoff, total suspended solids). As such, the role of weathering in consuming CO_2 appears substantial.

The importance of geochemical weathering as a CO_2 sink in high-mountain areas is well described (Hilton and West, 2020; Donnini et al., 2016), where rapid weathering of carbonate and silicate rock consumes CO_2. In particular, elevated rates of weathering are expected for subglacial environments, where water flows over recently crushed, fine-grained reactive mineral surfaces (Tranter, 2003; Sharp et al., 1995). This process can continue in proglacial streams, where suspended sediments with high surface areas promote continued CO_2 drawdown (St. Pierre et al., 2019). Indeed, we see the lowest CO_2 saturation at the two most glacially influenced streams (VAU and VAD) within the Valsorey catchment. Glacially enhanced weathering thus appears significant in this study as well.

Still, with periods of CO_2 undersaturation in all our study catchments, geochemical weathering appears to be relevant regardless of the presence of the glacier. To further constrain weathering as the primary sink of CO_2 in these catchments, we can also assess the potential for carbon fixation via photosynthesis as an alternative cause of undersaturation. With oxygen saturation consistently near or below saturation in all streams, photosynthesis is an unlikely driver of CO_2 undersaturation, as oxygen must inherently be above saturation to balance carbon fixation. Productivity has been shown to be limited in these streams outside of small temporal windows of opportunity (Boix Canadell et al., 2021), further reducing the likelihood. Lastly, the lack of variability in oxygen saturation across streams suggests photosynthetic rates do not vary significantly across streams, thus cannot account for the observed variability in CO_2 saturation.

In contrast, variability within the DIC isotopic data does help explain the contribution of CO_2 to streams derived from the oxidation of organic matter in the terrestrial environment. The effect of organic carbon oxidation on δ^{13}C-DIC values is depletion, i.e., more negative values (Pawellek and Veizer, 1994). It is thus likely the depleted δ^{13}C-DIC values observed at the Champéry streams are a result of greater rates of organic carbon oxidation, where the pool of organic carbon is evinced by the high vegetation cover and stream DOC concentration. We can more narrowly identify this process as most likely occurring in catchment soils, as the near-equilibrium nature of oxygen and the relatively low concentrations of DOC suggests a minor role for in-stream respiration (Bernhardt et al., 2017). Stream CO_2 is generally supported by external sources of CO_2 such as soil respiration (Hotchkiss et al., 2015; Campeau et al., 2019), and has been shown for mountain streams in particular (Clow et al., 2021; Crawford et al., 2015). Thus, as soils develop and organic carbon accumulates, the potential for terrestrially derived CO_2 inputs to the stream increases and CO_2 saturation increases (Marx et al., 2017).The role of the terrestrial environment in affecting stream CO_2 saturation if reinforced by the PLS model, which selected both vegetation cover and DOC concentration as influential variables. As such, there appears to be a link between increasing CO_2 saturation in these streams and organic matter accumulation and processing in the terrestrial environment.

Given the importance of geochemical weathering to the carbon dynamics of these catchments, consideration of geological variability between sites is necessary. While major lithologies are dissimilar across sites (Table 1), the ratios of major ions are remarkably similar and highlight the importance of carbonate weathering across all sites (Figure 3). While carbonate-containing lithologies are clear in three of the catchments (Vallon de Nant, Champéry, Val Ferret), the carbonate-like signal in the Valsorey area is likely explained by high levels of calcite in the blue-grey schists (Bucher et al., 2017). This schist is primarily located beneath and near the glacier (Burri et al., 1999), thus glacier-enhanced weathering may disproportionately affect the weathering of this mineral. The prominence of carbonate weathering in these study streams may also indicate that the potential for geochemical weathering to serve as a CO_2 sink is elevated compared to glacier-fed streams globally (Torres et al., 2017). That is, catchments with lower proportions of carbonate-containing lithologies likely have lower potential as geochemical CO_2 sinks (St. Pierre et al., 2019). This elevated weathering as a result of carbonate-rich lithology is exemplified by the tributary stream in the Val Ferret catchment (Figure 3). Despite no glacier coverage within this subcatchment, the median CO_2 saturation is undersaturated (Table 2). This is likely explained by the abundance of limestone deposits, which weather relatively quickly and geochemically consume CO_2. In expanding these analyses of carbon to other regions and mountain ranges, direct geologic perspectives will be needed to differentiate potential geochemical weathering rates (Hilton and West, 2020), and hence the potential for CO_2 consumption.

4.3 Conceptual model of carbon budgets in glacierized catchments

Altogether, these results provide the basis of a simple conceptual model explaining contributions to stream CO_2, thereby explaining saturation dynamics across glacier, soil, and elevation gradients in mountain catchments (Figure 6). Across the entire range of elevation, geochemical weathering acts as a sink of CO_2 (Crawford et al., 2019), where the intensity of this sink is dependent in large part on catchment geology. Where present, glaciers can provide additional weathering potential, whereby higher concentrations of suspended sediment increase mineral surface area greatly (St. Pierre et al., 2019). Moreover, this elevated weathering potential can extend far downstream depending on the suspension and transport of glacial till. Decreasing glacier influence reduces total weathering potential, but CO_2 undersaturation as a result of weathering is not limited to glacierized catchments. With the development of soils within the catchment, inputs of allochthonous organic carbon and CO_2 increases, elevating CO_2 concentrations. This CO_2 likely derives primarily from soil respiration rather than in-stream respiration of organic carbon (Clow et al., 2021; Singer et al., 2012).

Figure 6: Conceptual model of processes affecting CO_2 saturation, and thus direction of flux, across glacier, soil, and elevation gradients within glacierized catchments. Geochemical weathering is important across the entire landscape, but is enhanced under glaciated conditions and nearness to the glacier. As vegetation and soil develop at lower elevation, terrestrial inputs add CO_2 through direct inputs from soil respiration and from organic carbon inputs which fuel in-stream respiration. The net balance of these processes determines the CO_2 saturation. In the aerial image of the Valsorey catchment, the transition from glacier to vegetation cover can be seen directly (from Google Earth 2023).

Estimated fluxes of dissolved carbon constituents further support this conceptual model and the dominant role of terrestrial processes in determining the relative balance within and between streams. First, the dominance of CO_2 to the absolute total flux emphasizes the significance of gaseous carbon effluxes across within river networks. Our result of 67%

contribution from CO_2 is similar to a study of a boreal catchment in Sweden, in which CO_2 accounted for 53% of the net carbon flux (Wallin et al., 2013). Similarly, In a glaciated catchment in Alaska (St. Pierre et al., 2019), the areal rate of CO_2 flux was found to be -0.38 g C m^{-2} catchment area d^{-1}, an order of magnitude higher than our most highly glaciated system (-0.03 g C m^{-2} catchment area d^{-1} at VAU). Following our conceptual model, the difference is explained by the much more heavily glaciated area of the Alaskan catchment (> 40%) and the limitation of the sampling period to the most intense glacial melt period (June – August). When glacier influence is highest, the potential for weathering is highest as well, driving consumption of CO_2. Yet, even without glacier influence, consumption of CO_2 through weathering is still possible within the catchment and should be considered in montane stream carbon budgets.

DIC contributes 29% to the total carbon flux, DOC contributes the least, generally indicating a greater influence of mineral processes rather than organic (Rehn et al., 2022). The low contribution of DOC differs greatly from the Swedish boreal catchment, where DOC contributed roughly 40% on average (Wallin et al., 2013). This difference not only highlights the limited soil development within high-mountain systems, but also the potential for increased DOC export to the stream with continued soil development. Nonetheless, as DOC contribution clearly increased with additional vegetation cover across our study systems, the role of the terrestrial landscape in supporting stream organic carbon content is clear.

Our focus on broad relationships across these 12 locations recognizably conceals how local conditions and seasonality may affect site specific dynamics. Previous analyses have examined CO_2 and DOC individually at these stream locations, and provide some perspective. On a finer spatial scale within the stream network, local groundwater inputs can disproportionately elevate CO_2 concentration (Horgby et al., 2019b), which could be a useful tool in more directly quantifying terrestrial inputs to streams. Seasonally, the clearest pattern of pCO_2 indicates elevated contributions of terrestrial CO_2 during the spring snowmelt (Horgby et al., 2019a). Further differentiating temporal patterns during shorter timescales, such as storm events, may be useful in elucidating the contribution of soil respiration to the streams (Marzolf et al., 2022). While there is surely more to be learned at these finer spatial and temporal scales of both organic and inorganic carbon, our focus on broad scale patterns across catchments allows us to make more generalizable conclusions. Given the strength of the observed relationships within our analyses and their consistency with other studies of high-mountain streams, our conceptual model provides a simple, yet important foundation with which to assess carbon dynamics in montane streams globally.

5. Conclusion

The organic and inorganic components of the dissolved carbon pool shift across a glacier and vegetation gradient, driven by the relative balance of geochemical weathering and terrestrial carbon inputs to the stream. Our results also highlight an expanded importance of geochemical weathering in high-mountain ecosystems globally, whereby carbonate and silicate weathering may consume CO_2 across more mountain landscapes than previously considered (Horgby et al., 2019c). Implications for landscape carbon balances are clear, with decreased potential for CO_2 uptake and increased emissions of terrestrially-derived CO_2 emerging after glacier retreat and landscape greening. The rate of the transition from carbon sink to source is likely accelerated by climate change (Knight and Harrison, 2014), thus continued examination of the contributions of these processes to net stream balances is critical to predicting the future role of mountain catchments in the global carbon cycle.

Data availability

Data used in this analysis is available through the METALP data portal (https://metalp-data.epfl.ch/) or through publicly accessible university and government portals (e.g., http://www.climate.unibe.ch or http://map.geo.admin.ch).

Author contributions

TB secured funding for the research. ND and CR performed field and laboratory analyses. AR, ND, CR, and NM processed and analyzed the results. AR conducted statistical analyses. ND performed geospatial analyses. AR led manuscript development and revised the manuscript with input from all co-authors.

Competing interests

The authors declare that they have no conflict of interest.

Acknowledgements

The research leading to these results has received funding from the Swiss Science Foundation grant agreement 200021_163015 (METALP project). We thank Dr. Hannes Peter for assistance in analyzing the fluorescent properties of dissolved organic matter and for providing feedback in manuscript development. We also acknowledge members of the RIVER lab for assistance in field work and laboratory analyses.

References

Anderson, S. P., Drever, J. I., and Humphrey, N. F.: Chemical weathering in glacial environments, Geology, 25, 399–402, https://doi.org/10.1130/0091-7613(1997)025<0399:CWIGE>2.3.CO, 1997.

Begum, M. S., Park, J. H., Yang, L., Shin, K. H., and Hur, J.: Optical and molecular indices of dissolved organic matter for estimating biodegradability and resulting carbon dioxide production in inland waters: A review, Water Res., 228, 119362, https://doi.org/10.1016/j.watres.2022.119362, 2023.

Beniston, M., Farinotti, D., Stoffel, M., Andreassen, L. M., Coppola, E., Eckert, N., Fantini, A., Giacona, F., Hauck, C., Huss, M., Huwald, H., Lehning, M., López-Moreno, J. I., Magnusson, J., Marty, C., Morán-Tejéda, E., Morin, S., Naaim, M., Provenzale, A., Rabatel, A., Six, D., Stötter, J., Strasser, U., Terzago, S., and Vincent, C.: The European mountain cryosphere: A review of its current state, trends, and future challenges, Cryosphere, 12, 759–794, https://doi.org/10.5194/tc-12-759-2018, 2018.

Bergstrom, A., Koch, J. C., O'Nee, S., and Baker, E.: Seasonality of solute flux and water source chemistry in a coastal glacierized watershed undergoing rapid change: Wolverine Glacier watershed, Alaska, Water Resour. Res., 57, e2020WR028725, https://doi.org/10.1029/2020WR028725, 2021.

Bernhardt, E. S., Heffernan, J. B., Grimm, N. B., Stanley, E. H., Harvey, J. W., Arroita, M., Appling, A. P., Cohen, M. J., Mcdowell, W. H., Hall, R. O., Read, J. S., Roberts, B. J., Stets, E. G., and Yackulic, C. B.: The metabolic regimes of flowing waters, Limnol. Oceanogr., 63,S99–S118, https://doi.org/10.1002/lno.10726, 2018.

Boix Canadell, M., Escoffier, N., Ulseth, A. J., Lane, S. N., and Battin, T. J.: Alpine glacier shrinkage drives shift in dissolved organic carbon export from quasi-chemostasis to transport limitation, Geophys. Res. Lett., 46, 8872–8881, https://doi.org/10.1029/2019GL083424, 2019.

Boix Canadell, M., Gómez-Gener, L., Clémençon, M., Lane, S. N., and Battin, T. J.: Daily entropy of dissolved oxygen reveals different energetic regimes and drivers among high-mountain stream types, Limnol. Oceanogr., 66, 1594–1610, https://doi.org/10.1002/lno.11670, 2020.

Boix Canadell, M., Gómez-Gener, L., Ulseth, A. J., Clémençon, M., Lane, S. N., and Battin, T. J.: Regimes of primary production and their drivers in Alpine streams, Freshw. Biol., 66, 1449–1463, https://doi.org/10.1111/fwb.13730, 2021.

Boyer, E. W., Hornberger, G. M., Bencala, K. E., and McKnight, D. M.: Response characteristics of DOC flushing in an alpine catchment, Hydrol. Process., 11, 1635–1647, https://doi.org/10.1002/(SICI)1099-1085(19971015)11:12<1635::AID-HYP494>3.0.CO;2-H, 1997.

Brighenti, S., Tolotti, M., Bruno, M. C., Wharton, G., Pusch, M. T., and Bertoldi, W.: Ecosystem shifts in Alpine streams under glacier retreat and rock glacier thaw: A review, Sci. Total Environ., 675, 542–559, https://doi.org/10.1016/j.scitotenv.2019.04.221, 2019.

Bucher, K., Zhou, W., and Strober, I.: Rocks control the chemical composition of surface water from the high Alpine Zermatt area (Swiss Alps), Swiss J. Geosci., 110, 811–831, https://doi.org/10.1007/s00015-017-0279-y, 2017.

Burri, M., Allimann, M., Chessex, R., Piaz, G. V. D., Valle, G. Della, Bois, L. Du, Gouffon,

Y., Guermani, A., Hagen, T., Krummenacher, D., and Looser, M. . O.: Chanrion (CN 1346) including Mont Vélan (CN 1366), in: Geological Atlas of Switzerland 1:25000. Bundesamt für Landestopografie swisstopo, edited by: Burri, M., Piaz, G. V. D., Valle, G. Della, Gouffon, Y., and Guermani, A., 1999.

Campeau, A., Bishop, K., Amvrosiadi, N., Billett, M. F., Garnett, M. H., Laudon, H., Öquist, M. G., and Wallin, M. B.: Current forest carbon fixation fuels stream CO_2 emissions, Nat. Commun., 10, 1876, https://doi.org/10.1038/s41467-019-09922-3, 2019.

Carrascal, L. M., Galván, I., and Gordo, O.: Partial least squares regression as an alternative to current regression methods used in ecology, Oikos, 118, 681–690, https://doi.org/10.1111/j.1600-0706.2008.16881.x, 2009.

Clow, D. W., Striegl, R. G., and Dornblaser, M. M.: Spatiotemporal dynamics of CO_2 gas exchange from headwater mountain streams, J. Geophys. Res. Biogeosciences, 126, e2021JG006509, https://doi.org/10.1029/2021JG006509, 2021.

Coble, P. G., Greent, S. A., Blought, N. V, and Gagosiant, R. B.: Characterization of dissolved organic matter in the Black Sea by fluorescence spectroscopy, Nature, 348, 432–435, https://doi.org/doi.org/10.1038/348432a0, 1990.

Coble, P. G., Castillo, C. E. Del, and Avril, B.: Distribution and optical properties of CDOM in the Arabian Sea during the 1995 Southwest Monsoon, Deep Sea Res. Part II Top. Stud. Oceanogr., 45, 2195–2223, https://doi.org/10.1016/S0967-0645(98)00068-X, 1998.

Colombo, N., Bocchiola, D., Martin, M., Confortola, G., Salerno, F., Godone, D., D'Amico, M. E., and Freppaz, M.: High export of nitrogen and dissolved organic carbon from an Alpine glacier (Indren Glacier, NW Italian Alps), Aquat. Sci., 81, 1–13, https://doi.org/10.1007/s00027-019-0670-z, 2019.

Crawford, J. T., Dornblaser, M. M., Stanley, E. H., Clow, D. W., and Striegl, R. G.: Source limitation of carbon gas emissions in high-elevation mountain streams and lakes, J. Geophys. Res. Biogeosciences, 120, 952–964, https://doi.org/10.1002/2014JG002861, 2015.

Crawford, J. T., Hinckley, E. L. S., Litaor, M. I., Brahney, J., and Neff, J. C.: Evidence for accelerated weathering and sulfate export in high alpine environments, Environ. Res. Lett., 14, 124092, https://doi.org/10.1088/1748-9326/ab5d9c, 2019.

Deluigi, N., Lambiel, C., and Kanevski, M.: Data-driven mapping of the potential mountain permafrost distribution, Sci. Total Environ., 590–591, 370–380, https://doi.org/10.1016/j.scitotenv.2017.02.041, 2017.

Donnini, M., Frondini, F., Probst, J. L., Probst, A., Cardellini, C., Marchesini, I., and Guzzetti, F.: Chemical weathering and consumption of atmospheric carbon dioxide in the Alpine region, Glob. Planet. Change, 136, 65–81, https://doi.org/10.1016/j.gloplacha.2015.10.017, 2016.

Duarte, C. M. and Prairie, Y. T.: Prevalence of heterotrophy and atmospheric CO_2 emissions from aquatic ecosystems, Ecosystems, 8, 862–870, https://doi.org/10.1007/s10021-005-0177-4, 2005.

Dümig, A., Smittenberg, R., and Kögel-knabner, I.: Concurrent evolution of organic and mineral components during initial soil development after retreat of the Damma glacier , Switzerland, Geoderma, 163, 83–94, https://doi.org/10.1016/j.geoderma.2011.04.006, 2011.

Egli, M., Mavris, C., Mirabella, A., and Giaccai, D.: Soil organic matter formation along a

738 chronosequence in the Morteratsch proglacial area (Upper Engadine, Switzerland), Catena,
739 82, 61–69, https://doi.org/10.1016/j.catena.2010.05.001, 2010.

740 Eriksson, L., Johansson, E., Kettaneh-Wold, N., and Wold, S.: Multi-and megavariate data
741 analysis: Principles and applications., Umetrics AB, Umeå, Sweden, 2001.

742 Fasching, C., Ulseth, A. J., Schelker, J., Steniczka, G., and Battin, T. J.: Hydrology controls
743 dissolved organic matter export and composition in an Alpine stream and its hyporheic zone,
744 Limnol. Oceanogr., 61, 558–571, https://doi.org/10.1002/lno.10232, 2016.

745 Fellman, J. B., Spencer, R. G. M., Hernes, P. J., Edwards, R. T., D'Amore, D. V., and Hood,
746 E.: The impact of glacier runoff on the biodegradability and biochemical composition of
747 terrigenous dissolved organic matter in near-shore marine ecosystems, Mar. Chem., 121, 112–
748 122, https://doi.org/10.1016/j.marchem.2010.03.009, 2010.

749 Finstad, A. G., Andersen, T., Larsen, S., Tominaga, K., and Blumentrath, S.: From greening
750 to browning: Catchment vegetation development and reduced S-deposition promote organic
751 carbon load on decadal time scales in Nordic lakes, Sci. Rep., 6, 31944,
752 https://doi.org/10.1038/srep31944, 2016.

753 Garcia, R. D., Reissig, M., Queimaliños, C. P., Garcia, P. E., and Dieguez, M. C.: Climate-
754 driven terrestrial inputs in ultraoligotrophic mountain streams of Andean Patagonia revealed
755 through chromophoric and fluorescent dissolved organic matter, Sci. Total Environ., 521–522,
756 280–292, https://doi.org/10.1016/j.scitotenv.2015.03.102, 2015.

757 Gómez-Gener, L., Hotchkiss, E. R., Laudon, H., and Sponseller, R. A.: Integrating discharge-
758 concentration dynamics across carbon forms in a boreal landscape, Water Resour. Res., 57, 1–
759 18, https://doi.org/10.1029/2020WR028806, 2021.

760 Gordon, N. D., McMahon, T. A., Finlayson, B. L., Gippel, C. J., and Nathan, R. J.: Stream
761 hydrology: an introduction for ecologists, John Wiely and Sons, 2004.

762 Guelland, K., Hagedorn, F., Smittenberg, R. H., Goransson, H., Bernasconi, S. M., Hajdas, I.,
763 and Kretzschmar, R.: Evolution of carbon fluxes during initial soil formation along the
764 forefield of Damma glacier, Switzerland, Biogeochemistry, 113, 545–561,
765 https://doi.org/10.1007/s10533-012-9785-1, 2013.

766 Guillemette, F. and del Giorgio, P. A.: Simultaneous consumption and production of
767 fluorescent dissolved organic matter by lake bacterioplankton, Environ. Microbiol., 14, 1432–
768 1443, https://doi.org/10.1111/j.1462-2920.2012.02728.x, 2012.

769 Hagedorn, F., Gavazov, K., and Alexander, J. M.: Above- and belowground linkages shape
770 responses of mountain vegetation to climate change, Science, 365, 1119–1123,
771 https://doi.org/10.1126/science.aax4737, 2019.

772 Hall, R. O., Tank, J. L., Baker, M. A., Rosi-Marshall, E. J., and Hotchkiss, E. R.: Metabolism,
773 gas exchange, and carbon spiraling in rivers, Ecosystems, 19, 73–86,
774 https://doi.org/10.1007/s10021-015-9918-1, 2016.

775 Henne, P. D., Elkin, C. M., Reineking, B., Bugmann, H., and Tinner, W.: Did soil
776 development limit spruce (Picea abies) expansion in the Central Alps during the Holocene?
777 Testing a palaeobotanical hypothesis with a dynamic landscape model, J. Bio, 38, 933–949,
778 https://doi.org/10.1111/j.1365-2699.2010.02460.x, 2011.

779 Hilton, R. G. and West, A. J.: Mountains, erosion and the carbon cycle, Nat. Rev. Earth
780 Environ., 1, 284–299, https://doi.org/10.1038/s43017-020-0058-6, 2020.

781 Hodson, A., Tranter, M., and Vatne, G.: Contemporary rates of chemical denudation and
782 atmospheric CO_2 sequestration in glacier basins: an Arctic perspective, Earth Surf. Process.
783 Landforms, 25, 1447–1471, https://doi.org/10.1002/1096-9837(200012)25:13<1447::AID-
784 ESP156>3.0.CO;2-9, 2000.

785 Hoffmann, U., Hoffmann, T., Jurasinski, G., Glatzel, S., and Kuhn, N. J.: Assessing the
786 spatial variability of soil organic carbon stocks in an alpine setting (Grindelwald, Swiss Alps),
787 Geoderma, 232–234, 270–283, https://doi.org/10.1016/j.geoderma.2014.04.038, 2014.

788 Hongve, D., Riise, G., and Kristiansen, J. F.: Increased colour and organic acid concentrations
789 in Norwegian forest lakes and drinking water – a result of increased precipitation?, Aquat.
790 Sci., 66, 231–238, https://doi.org/10.1007/s00027-004-0708-7, 2004.

791 Hood, E., Fellman, J., Spencer, R. G. M., Hernes, P. J., Edwards, R., Damore, D., and Scott,
792 D.: Glaciers as a source of ancient and labile organic matter to the marine environment,
793 Nature, 462, 1044–1047, https://doi.org/10.1038/nature08580, 2009.

794 Horgby, Å., Gómez-Gener, L., Escoffier, N., and Battin, T. J.: Dynamics and potential drivers
795 of CO_2 concentration and evasion across temporal scales in high-alpine streams, Environ. Res.
796 Lett., 14, 124082, https://doi.org/10.1088/1748-9326/ab5cb8, 2019a.

797 Horgby, Å., Boix Canadell, M., Ulseth, A. J., Vennemann, T. W., and Battin, T. J.: High-
798 resolution spatial sampling identifies groundwater as driver of CO_2 dynamics in an alpine
799 stream network, J. Geophys. Res. Biogeosciences, 124, 1961–1976,
800 https://doi.org/10.1029/2019JG005047, 2019b.

801 Horgby, Å., Segatto, P. L., Bertuzzo, E., Lauerwald, R., Lehner, B., Ulseth, A. J.,
802 Vennemann, T. W., and Battin, T. J.: Unexpected large evasion fluxes of carbon dioxide from
803 turbulent streams draining the world's mountains, Nat. Commun., 10, 4888,
804 https://doi.org/10.1038/s41467-019-12905-z, 2019c.

805 Hotchkiss, E. R., Hall Jr, R. O., Sponseller, R. A., Butman, D., Klaminder, J., Laudon, H.,
806 Rosvall, M., and Karlsson, J.: Sources of and processes controlling CO_2 emissions change
807 with the size of streams and rivers, Nat. Geosci., 8, 696–699,
808 https://doi.org/10.1038/ngeo2507, 2015.

809 Imbeau, E. and Vincent, W. F.: Hidden stores of organic matter in northern lake ice: selective
810 retention of terrestrial particles, phytoplankton and labile carbon, J. Geophys. Res.
811 Biogeosciences, 126, e2020JG006233, https://doi.org/10.1029/2020JG006233, 2021.

812 Kida, M., Kojima, T., Tanabe, Y., Hayashi, K., Kudoh, S., Maie, N., and Fujitake, N.: Origin,
813 distributions, and environmental significance of ubiquitous humic-like fluorophores in
814 Antarctic lakes and streams, Water Res., 163, 114901,
815 https://doi.org/10.1016/j.watres.2019.114901, 2019.

816 Kida, M., Fujitake, N., Kojima, T., Tanabe, Y., Hayashi, K., Kudoh, S., and Dittmar, T.:
817 Dissolved organic matter processing in pristine Antarctic streams, Environ. Sci. Technol., 55,
818 10175–10185, https://doi.org/10.1021/acs.est.1c03163, 2021.

819 Klaar, M. J., Kidd, C., Malone, E., Bartlett, R., Pinay, G., Chapin, F. S., and Milner, A.:
820 Vegetation succession in deglaciated landscapes : implications for sediment and landscape
821 stability, Earth Surf. Process. Landforms, 40, 1088–1100, https://doi.org/10.1002/esp.3691,
822 2014.

823 Kneib, M., Cauvy-Fraunié, S., Escoffier, N., Boix Canadell, M., Horgby, and Battin, T. J.:

824 Glacier retreat changes diurnal variation intensity and frequency of hydrologic variables in
825 Alpine and Andean streams, J. Hydrol., 583, 124578,
826 https://doi.org/10.1016/j.jhydrol.2020.124578, 2020.

827 Knight, J. and Harrison, S.: Mountain glacial and paraglacial environments under global
828 climate change: Lessons from the past, future directions and policy implications, Geogr. Ann.
829 Ser. A Phys. Geogr., 96, 245–264, https://doi.org/10.1111/geoa.12051, 2014.

830 Kritzberg, E. S., Hasselquist, E. M., Martin, S., Olsson, O., Stadmark, J., and Valinia, S.:
831 Browning of freshwaters: Consequences to ecosystem services, underlying drivers, and
832 potential mitigation measures, Ambio, 49, 375–390, https://doi.org/10.1007/s13280-019-
833 01227-5, 2019.

834 Lafrenière, M. J. and Sharp, M. J.: The concentration and fluorescence of dissolved organic
835 carbon (DOC) in glacial and nonglacial catchments: interpreting hydrological flow routing
836 and DOC sources, Arctic, Antarct. Alp. Res., 36, 156–165, https://doi.org/10.1657/1523-
837 0430(2004)036[0156:TCAFOD]2.0.CO;2, 2004.

838 Mackay, J. D., Barrand, N. E., Hannah, D. M., Krause, S., Jackson, C. R., Everest, J.,
839 Aoalgeirsdóttir, G., and Black, A.: Future evolution and uncertainty of river flow regime
840 change in a deglaciating river basin, Hydrol. Earth Syst. Sci., 23, 1833–1865,
841 https://doi.org/10.5194/hess-23-1833-2019, 2019.

842 Marx, A., Dusek, J., Jankovec, J., Sanda, M., Vogel, T., van Geldern, R., Hartmann, J., and
843 Barth, J. A. C.: A review of CO_2 and associated carbon dynamics in headwater streams: A
844 global perspective, Rev. Geophys., 55, 560–585, https://doi.org/10.1002/2016RG000547,
845 2017.

846 Marzolf, N. S., Small, G. E., Oviedo-Vargas, D., Ganong, C. N., Duff, J. H., Ramírez, A.,
847 Pringle, C. M., Genereux, D. P., and Ardón, M.: Partitioning inorganic carbon fluxes from
848 paired O_2-CO_2 gases in a headwater stream, Costa Rica, Biogeochemistry, 160, 259–273,
849 https://doi.org/10.1007/s10533-022-00954-4, 2022.

850 Massicotte, P.: eemR: tools for pre-processing emission-excitation-matrix (EEM)
851 fluorescence data, R Packag. version 1.0.1, 2019.

852 Masson-Delmotte, V., Zhai, P., Pirani, A., Connors, S. L., Péan, C., Berger, S., Caud, N.,
853 Chen, Y., Goldfarb, L., Gomis, M. I., Huang, M., Leitzell, K., Lonnoy, E., Matthews, J. B. R.,
854 Maycock, T. K., Waterfield, T., Yelekçi, O., Yu, R., and Zhou, B. (Eds.): Climate change
855 2021: The physical science basis. Working Group I contribution to the IPCC Sixth
856 Assessment Report, Cambridge University Press, Cambridge, United Kingdom and New
857 York, NY, USA, https://doi.org/10.1017/9781009157896, 2021.

858 Milner, A. M., Brown, L. E., and Hannah, D. M.: Hydroecological response of river systems
859 to shrinking glaciers, Hydrol. Process., 23, 62–77, https://doi.org/10.1002/hyp, 2009.

860 Milner, A. M., Khamis, K., Battin, T. J., Brittain, J. E., Barrand, N. E., Füreder, L., Cauvy-
861 Fraunié, S., Gíslason, G. M., Jacobsen, D., Hannah, D. M., Hodson, A. J., Hood, E., Lencioni,
862 V., Ólafsson, J. S., Robinson, C. T., Tranter, M., and Brown, L. E.: Glacier shrinkage driving
863 global changes in downstream systems, Proc. Natl. Acad. Sci. U. S. A., 114, 9770–9778,
864 https://doi.org/10.1073/pnas.1619807114, 2017.

865 Murphy, K. R., Butler, K. D., Spencer, R. G. M., Stedmon, C. A., Boehme, J. R., and Aiken,
866 G. R.: Measurement of dissolved organic matter fluorescence in aquatic environments: an
867 interlaboratory comparison, Environ. Sci. Technol., 44, 9405–9412,

https://doi.org/10.1021/es102362t, 2010.

Murphy, K. R., Stedmon, C. A., Graeber, D., and Bro, R.: Fluorescence spectroscopy and multi-way techniques. PARAFAC, Anal. Methods, 5, 6557, https://doi.org/10.1039/c3ay41160e, 2013.

Murphy, K. R., Stedmon, C. A., Wenig, P., and Bro, R.: OpenFluor – an online spectral library of auto- fl uorescence by organic compounds in the environment †, Anal. Methods, 6, 658–661, https://doi.org/10.1039/c3ay41935e, 2014.

Nash, M. S. and Chaloud, D. J.: Partial least square analyses of landscape and surface water biota sssociations in the Savannah River basin, ISRN Ecol., 2011, 1–11, https://doi.org/10.5402/2011/571749, 2011.

Onderka, M., Wrede, S., Rodný, M., Pfister, L., Hoffmann, L., and Krein, A.: Hydrogeologic and landscape controls of dissolved inorganic nitrogen (DIN) and dissolved silica (DSi) fluxes in heterogeneous catchments, J. Hydrol., 450–451, 36–47, https://doi.org/10.1016/j.jhydrol.2012.05.035, 2012.

Paillex, A., Siebers, A. R., Ebi, C., Mesman, J., and Robinson, C. T.: High stream intermittency in an alpine fluvial network: Val Roseg, Switzerland, Limnol. Oceanogr., 65, 557–568, https://doi.org/10.1002/lno.11324, 2020.

Pain, A. J., Martin, J. B., Martin, E. E., Rahman, S., and Ackermann, P.: Differences in the quantity and quality of organic matter exported from Greenlandic glacial and deglaciated watersheds, Global Biogeochem. Cycles, 34, 1–20, https://doi.org/10.1029/2020GB006614, 2020.

Pawellek, F. and Veizer, J.: Carbon cycle in the upper Danube and its tributaries: δ13C-DIC constraints, Isr. J. Earth Sci., 43, 187–194, 1994.

St. Pierre, K. A., St. Louis, V. L., Schiff, S. L., Lehnherr, I., Dainard, P. G., Gardner, A. S., Aukes, P. J. K., and Sharp, M. J.: Proglacial freshwaters are significant and previously unrecognized sinks of atmospheric CO_2, Proc. Natl. Acad. Sci. U. S. A., 116, 17690–17695, https://doi.org/10.1073/pnas.1904241116, 2019.

Plummer, L. N. and Busenberg, E.: The solubilities of calcite, aragonite and vaterite in CO_2-H2O solutions between 0 and 90°C, and an evaluation of the aqueous model for the system $CaCO_3$-CO_2-H_2O, Geochim. Cosmochim. Acta, 46, 1011–1040, https://doi.org/10.1016/0016-7037(82)90056-4, 1982.

Pucher, M., Wünsch, U., Weigelhofer, G., Murphy, K., Hein, T., and Graeber, D.: staRdom: versatile software for analyzing spectroscopic data of dissolved organic matter in R, Water, 11, 2366, https://doi.org/10.3390/w11112366, 2019.

Rehn, L., Sponseller, R. A., Laudon, H., and Wallin, M. B.: Long-term changes in dissolved inorganic carbon across boreal streams caused by altered hydrology, Limnol. Oceanogr., 68, 409–423, https://doi.org/10.1002/lno.12282, 2022.

Roulet, N. and Moore, T. R.: Browning the waters, Nature, 444, 283–284, https://doi.org/10.1038/444283a, 2006.

Rumpf, S. B., Gravey, M., Brönnimann, O., Luoto, M., Cianfrani, C., Mariethoz, G., and Guisan, A.: From white to green: Snow cover loss and increased vegetation productivity in the European Alps, Science, 376, 1119–1122, 2022.

Sharp, M., Tranter, M., Brown, G. H., and Skidmore, M.: Rates of chemical denudation and CO_2 drawdown in a glacier-covered alpine catchment, Geology, 23, 61–64, https://doi.org/10.1130/0091-7613(1995)023<0061:ROCDAC>2.3.CO;2, 1995.

Singer, G. A., Fasching, C., Wilhelm, L., Niggemann, J., Steier, P., Dittmar, T., and Battin, T. J.: Biogeochemically diverse organic matter in Alpine glaciers and its downstream fate, Nat. Geosci., 5, 710–714, https://doi.org/10.1038/ngeo1581, 2012.

Skidmore, M., Sharp, M., and Tranter, M.: Kinetic isotopic fractionation during carbonate dissolution in laboratory experiments : implications for detection of microbial CO 2 signatures using □ 13 C-DIC, Geochim. Cosmochim. Acta, 68, 4309–4317, https://doi.org/10.1016/j.gca.2003.09.024, 2004.

Spencer, R. G. M., Vermilyea, A., Fellman, J., Raymond, P., Stubbins, A., Scott, D., and Hood, E.: Seasonal variability of organic matter composition in an Alaskan glacier out flow: insights into glacier carbon sources, Environ. Res. Lett., 9, 055005, https://doi.org/10.1088/1748-9326/9/5/055005, 2014.

Stedmon, C. A. and Bro, R.: Characterizing dissolved organic matter fluorescence with parallel factor analysis: a tutorial, Limnol. Oceanogr. Fluids Environ., 6, 572–579, https://doi.org/10.4319/lom.2008.6.572, 2008.

Torres, M. A., Moosdorf, N., Hartmann, J., Adkins, J. F., and West, A. J.: Glacial weathering, sulfide oxidation, and global carbon cycle feedbacks, Proc. Natl. Acad. Sci. U. S. A., 114, 8716–8721, https://doi.org/10.1073/pnas.1702953114, 2017.

Tranter, M.: Geochemical weathering in glacial and proglacial environments, Treatise on Geochemistry, 5, 605, https://doi.org/10.1016/B0-08-043751-6/05078-7, 2003.

Ulseth, A. J., Hall, R. O., Boix Canadell, M., Madinger, H. L., Niayifar, A., and Battin, T. J.: Distinct air–water gas exchange regimes in low- and high-energy streams, Nat. Geosci., 12, 259–263, https://doi.org/10.1038/s41561-019-0324-8, 2019.

Wallin, M. B., Grabs, T., Buffam, I., Laudon, H., Ågren, A., Öquist, M. G., and Bishop, K.: Evasion of CO_2 from streams - The dominant component of the carbon export through the aquatic conduit in a boreal landscape, Glob. Chang. Biol., 19, 785–797, https://doi.org/10.1111/gcb.12083, 2013.

Wanninkhof, R.: Relationship between wind speed and gas exchange over the ocean revisited, Limnol. Oceanogr. Methods, 12, 351–362, https://doi.org/10.4319/lom.2014.12.351, 2014.

Wietrzyk-Pełka, P., Rola, K., Szymański, W., and Węgrzyn, M. H.: Organic carbon accumulation in the glacier forelands with regard to variability of environmental conditions in different ecogenesis stages of High Arctic ecosystems, Sci. Total Environ., 717, 1–12, https://doi.org/10.1016/j.scitotenv.2019.135151, 2020.

Wold, S., Ruhe, A., Wold, H., and Dunn III, W. J.: The collinearity problem in linear regression. The partial least squares (PLS) approach to generalized inverses, SIAM J. Sci. Stat. Comput., 5, 735–743, 1984.

Zah, R. and Uehlinger, U.: Particulate organic matter inputs to a glacial stream ecosystem in the Swiss Alps, Freshw. Biol., 46, 1597–1608, https://doi.org/10.1046/j.1365-2427.2001.00847.x, 2001.

Zhou, Y., Zhou, L., He, X., Jang, K. S., Yao, X., Hu, Y., Zhang, Y., Li, X., Spencer, R. G. M., Brookes, J. D., and Jeppesen, E.: Variability in dissolved organic matter composition and

biolability across gradients of glacial coverage and distance from glacial terminus on the Tibetan Plateau, Environ. Sci. Technol., 53, 12207–12217, https://doi.org/10.1021/acs.est.9b03348, 2019.

957 Table 1: Catchment characteristics.

Catchment	ID	Station	Station altitude (m a.s.l.)	Area (km^2)	Glacier coverage (%)	Vegetation coverage (%)	Dominant lithology
Valsorey	VAD	Down	1936	23.2	27.4	24.2	Blue-grey schists, gneiss, schist
	VAU	Up	2148	18.1	33.5	21.1	
	VEL	Tributary	2161	3.11	0	56.7	
Ferret	FED	Down	1773	20.2	3.41	62.4	Limestone, sandstone, schist
	FEU	Up	1996	9.33	7.40	46.3	
	PEU	Tributary	2024	3.97	0	70.2	
Vallon de Nant	AND	Down	1197	13.4	4.58	63.9	Limestone; calcareous shale; flysch
	AVU	Up	1465	8.99	6.80	54.0	
	RIC	Tributary	1192	14.3	6.38	64.2	
Champery	VID	Down	1416	3.64	0	94.0	Flysch, limestone; shale
	VIM	Middle	1630	0.74	0	86.1	
	VIU	Up	1689	0.31	0	80.9	

958

Table 2: Median concentration of DOC and DIC, percent saturation of CO_2 and O_2, and isotopic composition of DIC for the 12 sites. Concentration and isotopic composition are summarized from grab samples, while CO_2 and O_2 saturation are summarized from sensor data.

Catchment	Station	DOC (mg L^{-1})	DIC (mg L^{-1})	$CO_{2,sat}$ (%)	$O_{2,sat}$ (%)	δ^{13}C-DIC (‰)
Valsorey	Down	0.19	0.79	77.4	98.6	-5.34
	Up	0.17	0.80	68,1	99.0	-6.08
	Tributary	0.30	0.84	77.7	98.3	-6.57
Ferret	Down	0.18	1.82	90.7	99.3	-4.04
	Up	0.12	1.38	137	99.0	-3.98
	Tributary	0.15	1.93	97.0	99.5	-3.67
Vallon de Nant	Down	0.14	1.76	98.4	99.8	-5.10
	Up	0.13	1.79	123	99.0	-6.31
	Tributary	0.45	2.01	100	99.2	-6.96
Champery	Down	0.36	2.65	130	99.2	-8.45
	Middle	0.38	2.22	103	99.5	-9.29
	Up	0.31	2.13	96.2	98.8	-9.76

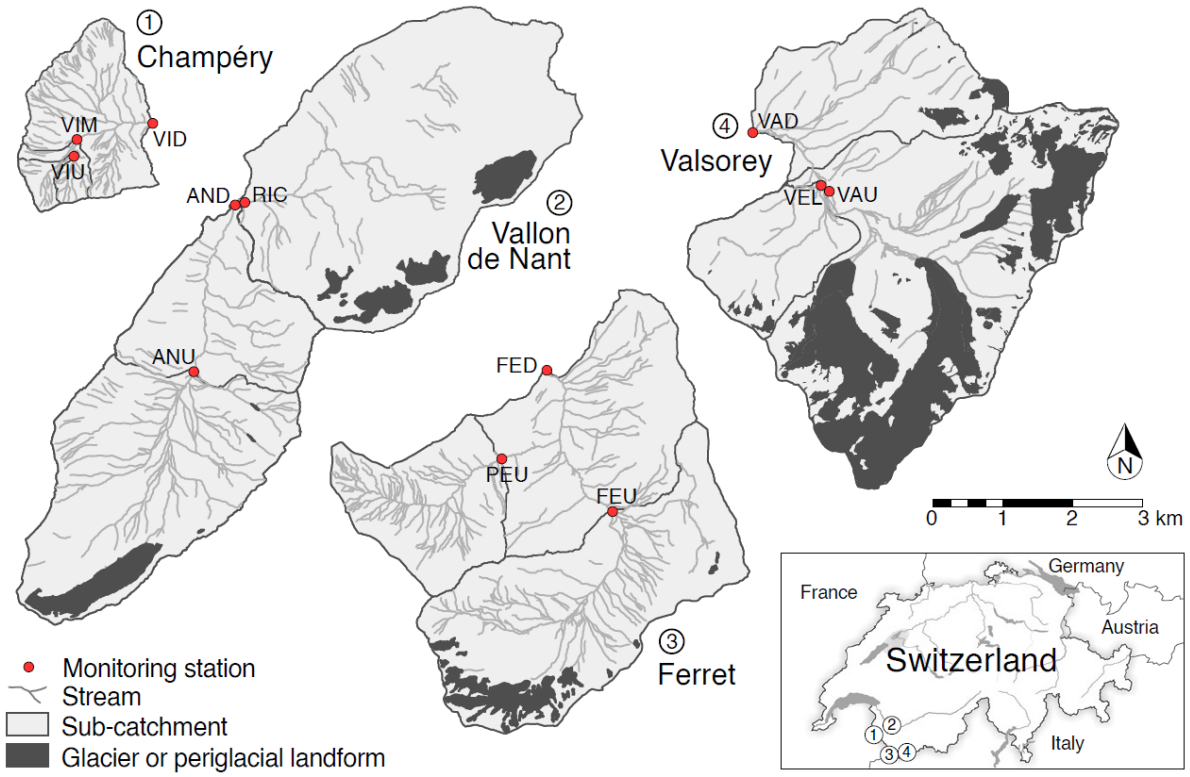

Figure 1: Map of the 12 study sites within four catchments of the Alps in southwestern Switzerland (glacial cover and stream network from swissTLM3D; swisstopo).

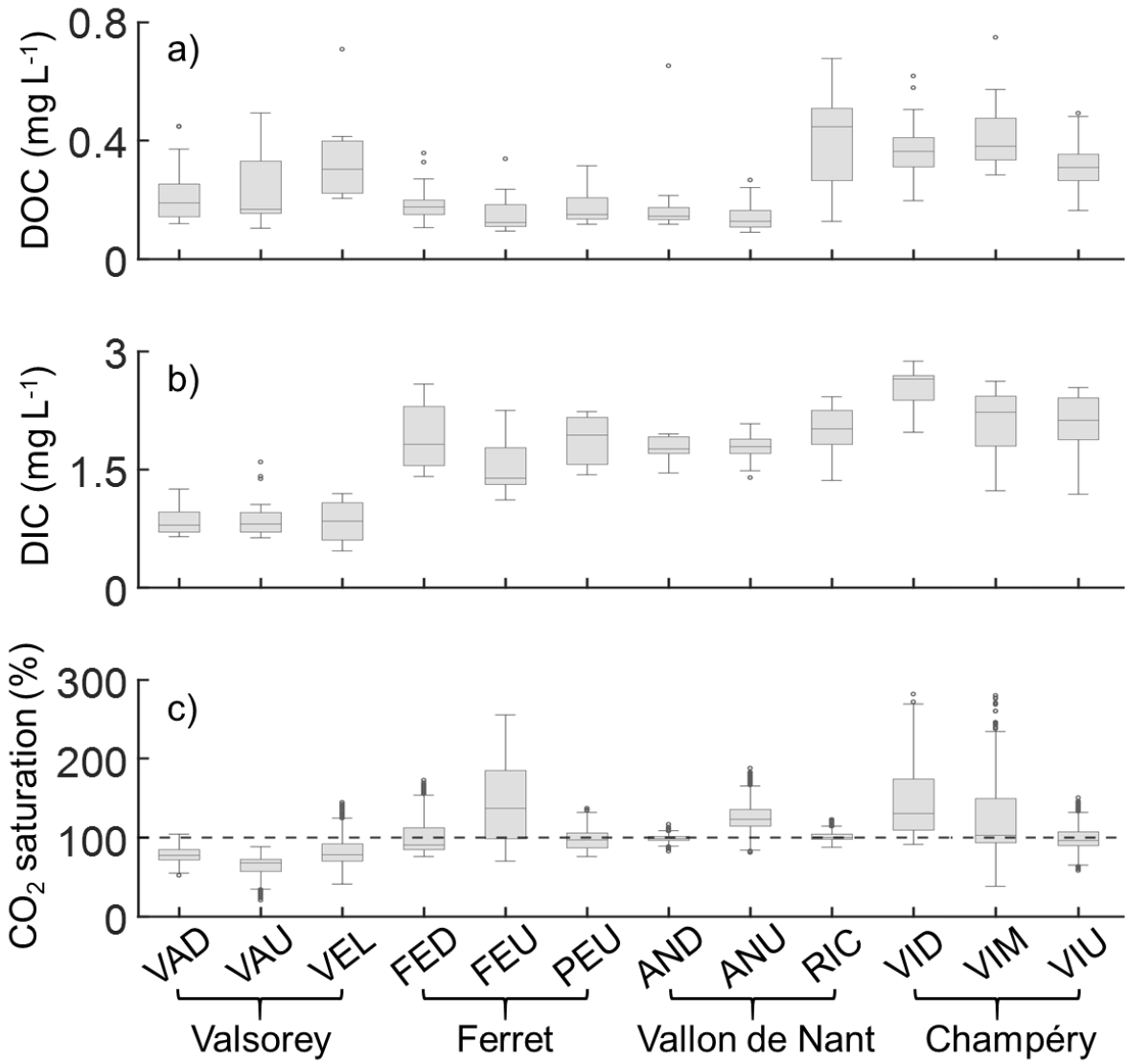

Figure 2: Boxplots of a) DOC and b) DIC concentration (mg L^{-1}) from grab samples, and c) CO_2 saturation (%) derived from sensor measurements.

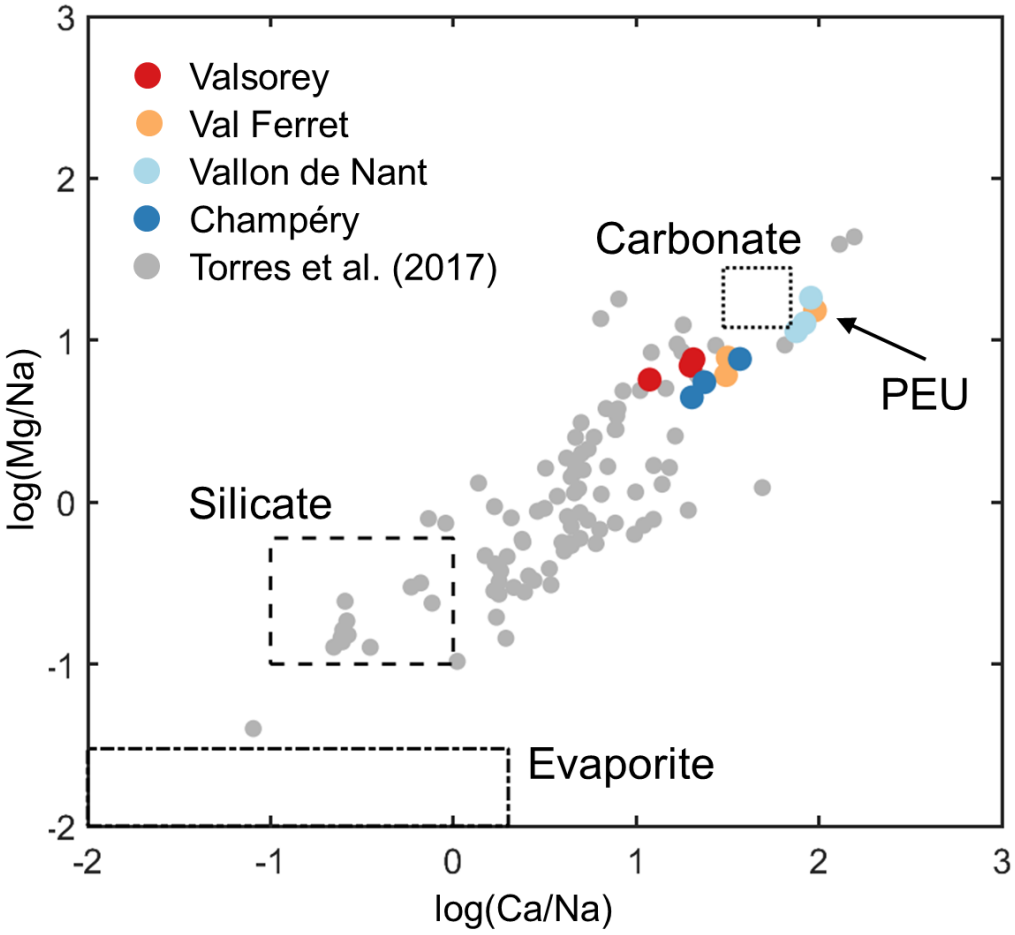

Figure 3: Stoichiometry of dissolved ion in the twelve study streams and a data base of 95 glacier-fed streams (Torres et al., 2017). The range of each lithological end-member are shown by the boxes. The tributary stream in the Val Ferret catchment (PEU) is shown as it is clearly distinguished from the main stream locations.

976

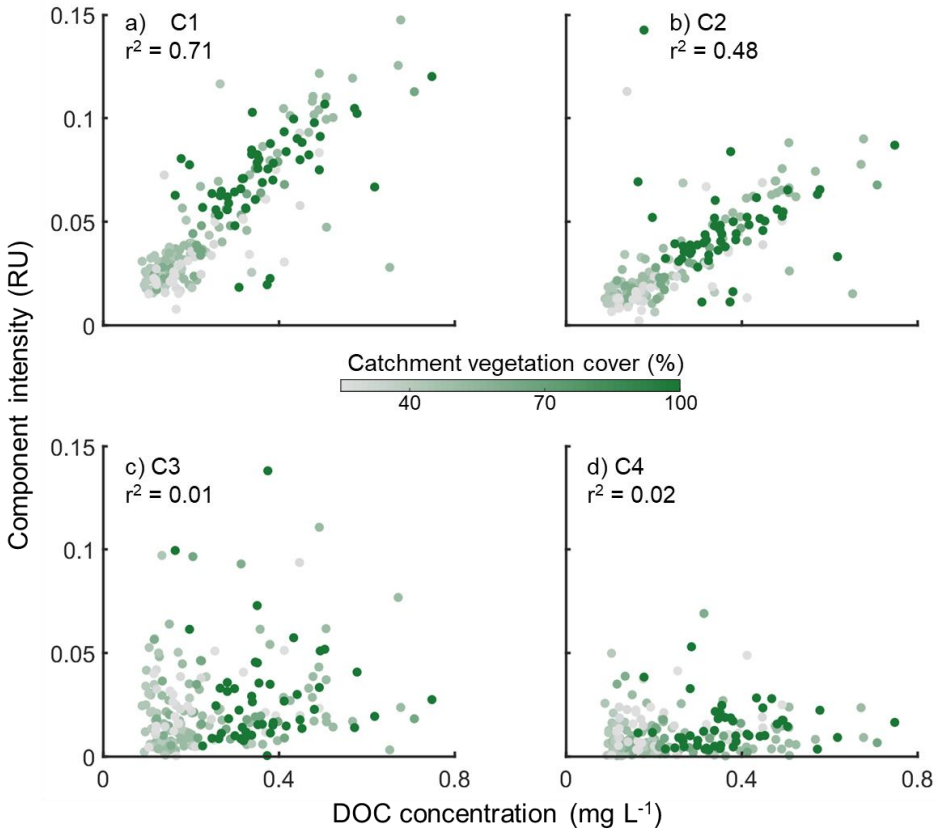

977
978 Figure 4: Intensity of the four components within the PARAFAC model against DOC
979 concentration from grab samples, with catchment vegetation cover shown by color. a)
980 Component 1 and b) component 2 represent humic-like compounds while c) component 3 and
981 d) component 4 represent proteinaceous compounds. The coefficient of determination (r^2) is
982 shown for each linear regression.

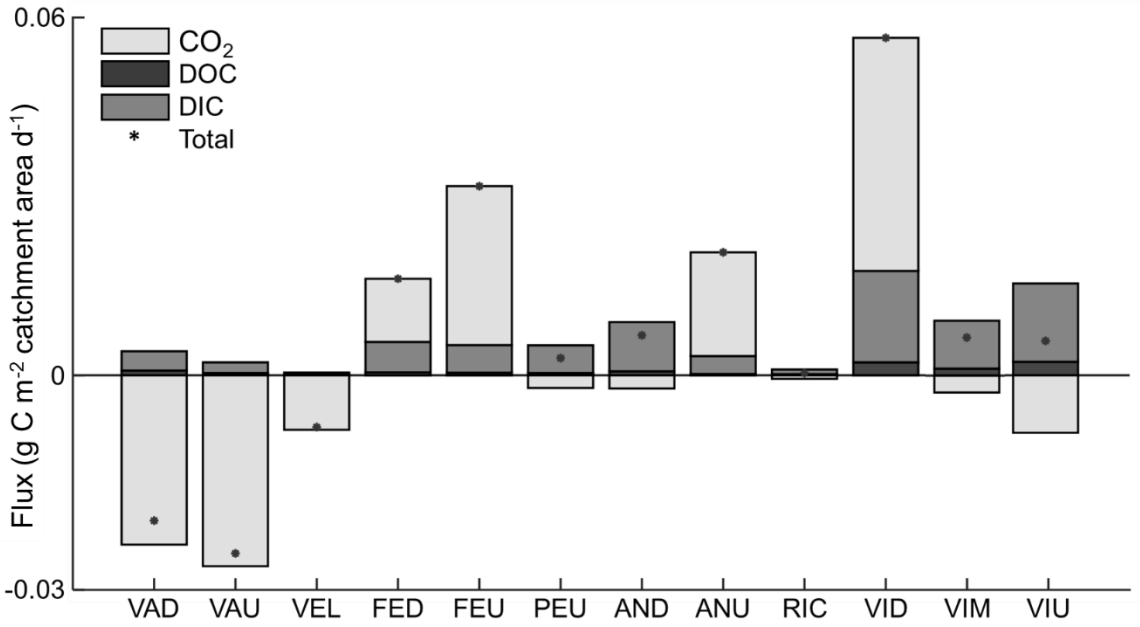

Figure 5: Estimated annual fluxes of the dissolved carbon components (CO_2, DOC, and DIC) normalized for catchment area.

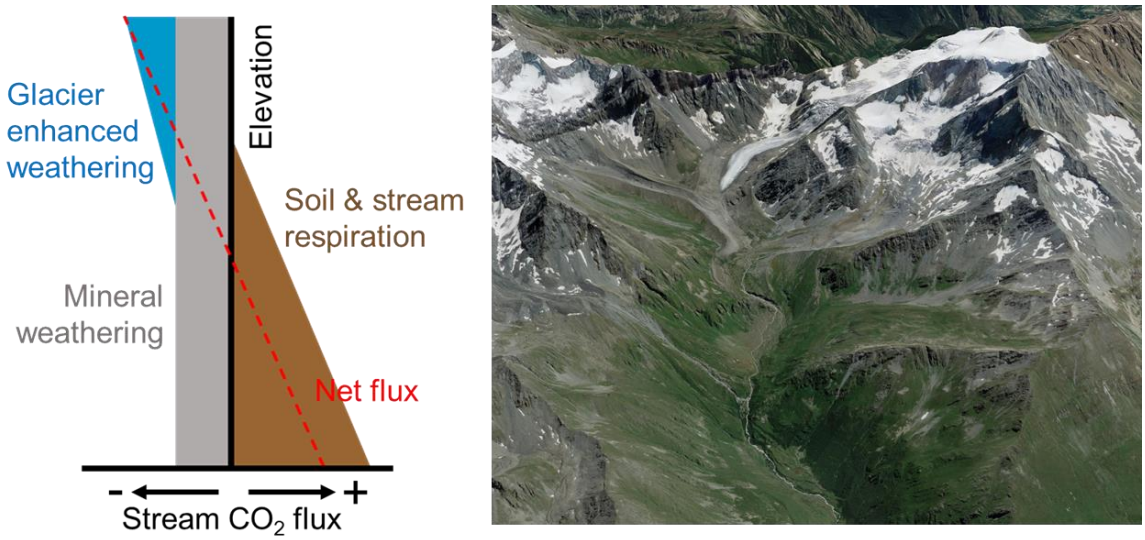

Figure 6: Conceptual model of processes affecting CO_2 saturation, and thus direction of flux, across glacier, soil, and elevation gradients within glacierized catchments. Geochemical weathering is important across the entire landscape, but is enhanced under glaciated conditions and nearness to the glacier. As vegetation and soil develop at lower elevation, terrestrial inputs add CO_2 through direct inputs from soil respiration and from organic carbon inputs which fuel in-stream respiration. The net balance of these processes determines the CO_2 saturation. In the aerial image of the Valsorey catchment, the transition from glacier to vegetation cover can be seen directly (from Google Earth 2023).